Application of SVM and BCG-FFT Method for the Parameter Reconstruction of Composite Conducting-Dielectric Cylinder

Q. H. Zhang and H. T. Chen

Department of Electronics and Information
Three Gorges University, Yichang, Hubei 443002, China
zhangqh020901@163.com, hbcht@126.com

Abstract **─** In this paper, Support Vector Machine (SVM) technique is used to reconstruct the geometric and dielectric characteristics of composite conducting-dielectric cylinder. To this aim, the scattered electric fields at a number of observation points by composite conducting-dielectric object under the different object parameters are calculated by stabilized Biconjugate Gradient Fast Fourier Transform method (BCG-FFT) and provide to SVM as input training samples, while the output of the SVM are the characteristics of the objects. In numerical results, the proposed technique is applied successfully to the reconstruction of the geometric and dielectric parameters of composite conducting-dielectric cylinder. The effectiveness of the SVM method is evaluated and also in comparison with the Neural Network (NN) based approaches.

Index Terms **─** Biconjugate Gradient Fast Fourier Transform (BCG-FFT), composite conducting-dielectric cylinder, parameter reconstruction and Support Vector Machine (SVM).

I. INTRODUCTION

The research on the characteristics of electromagnetic scattering has particular significance in aspects of Electromagnetic Compatibility (EMC), target properties, classification and identification, radar sense, etc. of electromagnetism. In recent years, the research on characteristics of scattering of objective metallic and dielectric composite structure (such as lossy medium covers conductor objective, micro-strip, micro-strip antenna, antenna-antenna housing system and so on) has been paid great attention to because of its wide application. So it is obvious that the research on its aspects of inverse scattering appears to be quite imperative and important.

As for the calculation of unitary problems in electromagnetic inverse scattering of composite conducting-dielectric objects, we can adopt several comparatively mature algorithms, such as the Method of Moment (MoM), the Finite Element Method (FEM), the Finite Difference Time Domain (FDTD), etc. In MoM, a typical computational method for this problem is based on the Surface Integral Equation formulation (SIE) [1] or the hybrid Volume-Surface Integral Equation (VSIE) formulation [2-4]. In comparison to the SIE approach, the VSIE approach has several unique advantages. First, the VSIE approach can conveniently handle composite objects with arbitrarily inhomogeneous dielectric materials due to the use of VSIE, while the SIE can only consider piecewise homogeneous dielectric materials. Besides, for composite conducting-dielectric targets, the SIE approach requires special treatments on the conducting-dielectric junctions to obtain accurate results [5]. On the other hand, the VSIE approach retains the same simple form, regardless of the complexity of the objects. Hence, the implementation is relatively convenient and simpler, as compared to the SIE approach. Also, no special treatments are required for problems with junctions. In this paper, we chose the VSIE to model the composite conducting-dielectric objects.

At present, there are so few documents and reports about the aspects of electromagnetic inverse scattering of metallic and dielectric composite structure object. As for traditional

Submitted On: September 23, 2012
Accepted On: January 19, 2014

optimization iteration method, on one hand, its calculation on unitary algorithm is more complex than the calculation on comparatively pure conductor or dielectric objective, because of the complexity of objective structure; on the other hand, the complexity of objective structure causes the more powerful nolinear of the aspects of inversing scattering. At the same time, we also need to pay more attention to the slowdown or convergence of iteration caused by the increasing number of object functions and optimization variables, it is time-consuming and certainly it will go against synchronous inversion towards objective.

In the last years, it's seen that the application research on the aspect of Artificial Neural Networks (ANN) in electromagnetic inverse scattering has already been started up; such as the free space on the basis of frequency domain or time domain information, the problem of electromagnetism inversing scattering of half-space buried-objects [6-10], etc. However, in spite of their success, NN-based approaches suffer from typical problems of neural networks (e.g., the overfitting, local minima, etc), which make the method accuracy highly training dependent.

In recent years, a new artificial intelligent technique-Support Vector Machine (SVM) has been proposed to solve electromagnetic inverse scattering problems. In [11] and [12], the SVM is used to the detection of buried object by frequency-domain data of scattered electric fields, combined with the Finite Element Method (FEM) and the Finite Difference Time Domain (FDTD) method, respectively. In particular, as in the case of the using of neural networks, SVM are used to estimate the unknown function that relates the scattering field to the target's properties. After a proper learning phase, the SVM can obtain reconstruction in real-time. Moreover, in SVM, the original problem is recasted into a Constrained Quadratic Programming (CQP) problem and it avoids typical drawbacks as overfitting or local minima occurrence [13].

This paper deals with the SVM-based reconstruction of composite conducting-dielectric objects starting from frequency-domain electromagnetic scattering data. To this aim, the stabilized Biconjugate Gradient Fast Fourier Transform method (BCG-FFT) is applied to solve the hybrid VSIE for composite conducting-dielectric cylinder, and the electromagnetic data exploitable for inversion are the amplitude of scattered fields collected at some receiving points.

II. THE MATHEMATICAL FORMULATION OF VSIE

Let's consider a mixed conducting and dielectric scattering target illuminated by an incident field $\boldsymbol{E}^i$. It is assumed that the dielectric materials are nonmagnetic, namely, $\mu=\mu_0$ for all regions and in the following formulation the time factor is $e^{j\omega t}$ and is suppressed. Using the equivalence principle, the conducting bodies are replaced by equivalent surface currents $\boldsymbol{J}_S$ and the dielectric materials are replaced by equivalent volume currents $\boldsymbol{J}_V$. All the currents radiate in free space, and hence the free-space Green's function is used in the formulation. The scattered field $\boldsymbol{E}^s$ is the total contribution of the surface current $\boldsymbol{J}_S$ and volume current $\boldsymbol{J}_V$, which can be calculated by [4]:

$$\boldsymbol{E}^s(\boldsymbol{r}) = -\mathrm{j}\omega\boldsymbol{A}_S(\boldsymbol{r}) - \nabla\Phi_S(\boldsymbol{r}) - \mathrm{j}\omega\boldsymbol{A}_V(\boldsymbol{r}) - \nabla\Phi_V(\boldsymbol{r}), \quad (1)$$

where $\boldsymbol{A}_S, \boldsymbol{A}_V, \Phi_S, \Phi_V$ are the vector and scalar potentials produced by the surface current $\boldsymbol{J}_S$ and volume current $\boldsymbol{J}_V$, respectively; and given by:

$$\boldsymbol{A}_u(\boldsymbol{r}) = \frac{\mu_0}{4\pi}\int_u \boldsymbol{J}_u(\boldsymbol{r}')\frac{e^{-jk_0|\boldsymbol{r}-\boldsymbol{r}'|}}{|\boldsymbol{r}-\boldsymbol{r}'|}\mathrm{d}u' \quad u = S, V, \quad (2)$$

$$\Phi_u(\boldsymbol{r}) = -\frac{1}{\mathrm{j}\omega 4\pi\varepsilon_0}\int_u \nabla\cdot\boldsymbol{J}_u(\boldsymbol{r}')\frac{e^{-jk_0|\boldsymbol{r}-\boldsymbol{r}'|}}{|\boldsymbol{r}-\boldsymbol{r}'|}\mathrm{d}u' \quad u = S, V. \quad (3)$$

On all conductor surfaces S, the boundary condition requires that the total tangential electric field is zero; i.e.:

$$\left\lfloor \boldsymbol{E}^{\mathrm{i}}(\boldsymbol{r}) + \boldsymbol{E}^s(\boldsymbol{r}) \right\rfloor_{\tan} = 0 \quad \boldsymbol{r} \in S. \quad (4)$$

This is the surface electric field integral equation. In the dielectric region, the total electric field is equal to the sum of the incident field and the scattered field; i.e.:

$$\boldsymbol{E}^{\mathrm{total}}(\boldsymbol{r}) = \boldsymbol{E}^{\mathrm{i}}(\boldsymbol{r}) + \boldsymbol{E}^{\mathrm{s}}(\boldsymbol{r}) \quad \boldsymbol{r} \in V, \quad (5)$$

the volume current $\boldsymbol{J}_V$ is related to the total electric field $\boldsymbol{E}^{\mathrm{total}}(\boldsymbol{r})$ by:

$$\boldsymbol{J}_V(\boldsymbol{r}) = \mathrm{j}\omega(\varepsilon(\boldsymbol{r}) - \varepsilon_0)\boldsymbol{E}^{\mathrm{total}}(\boldsymbol{r}) \quad \boldsymbol{r} \in V, \quad (6)$$

where $\varepsilon(\boldsymbol{r})$ is the permittivity of the dielectric material.

Put equation (5) into equation (6), the volume integral equation is given by:

$$\frac{\boldsymbol{J}_V(\boldsymbol{r})}{\mathrm{j}\omega(\varepsilon(\boldsymbol{r})-\varepsilon_0)}=\boldsymbol{E}^{\mathrm{i}}(\boldsymbol{r})+\boldsymbol{E}^{s}(\boldsymbol{r}) \quad \boldsymbol{r}\in V. \qquad (7)$$

Equations (4) and (7), together with (1)-(3), constitute a hybrid volume-surface integral equation in terms of the surface current $\boldsymbol{J}_S$ on the conducting surface and the volume current $\boldsymbol{J}_V$ in the dielectric region.

To solve the hybrid volume-surface integral equation, the conducting surface S is discretized into small quadrangle patches, while the dielectric region V is divided into hexahedron elements. However, the quadrangle-hexahedron mesh is not the only choice. Other types of meshes, such as triangular for surface and tetrahedral for volume can also be used. The unknown surface current $\boldsymbol{J}_S$ and volume current $\boldsymbol{J}_V$ can be represented by the pulse basis functions and be substituted into (4) and (7), testing a linear system consisting of independent equations is obtained and can be written as a sub-matrix form in the following:

$$\begin{bmatrix} Z_{SS} & Z_{SV} \\ Z_{VS} & Z_{VV} \end{bmatrix}\begin{bmatrix} I_{sn} \\ I_{vn} \end{bmatrix}=\begin{bmatrix} E^i_{sn} \\ E^i_{vn} \end{bmatrix}, \qquad (8)$$

where $Z_{tu}\,(u=S,V,t=S,V)$ is the impedance matrix, I_{sn}, I_{vn} are the expansion coefficient matrix of surface current and volume current, respectively and E^i_{sn}, E^i_{vn} are the electric voltage matrix of metal surface and dielectric internal, respectively. Once we get the surface current $\boldsymbol{J}_S$ and volume current $\boldsymbol{J}_V$ by matrix equation (8), we can get the scattering field of arbitrary point in space, as long as we put them into equation (1). Specifically, the numerical integration involved in the sub-matrix Z_{SS} and Z_{VV}, $a_t=\int_t G(\boldsymbol{r},\boldsymbol{r}')dt'$ ($t=S,V$), will show singularity when $\boldsymbol{r}=\boldsymbol{r}'$; i.e., the field point coincides with source point. To avoid this singularity, an approximate numerical method should be taken to yield accurate result. As for the surface integral, it can be solved approximately by solving the integral within the corresponding circular whose area is equal to rectangle in polar coordinate. In terms of volume integral, we use the integration of the sphere, which has the equal volume of the cube to obtain the numerical solution:

$$I_1=j\omega\mu_0[\frac{1}{k_0^2}(e^{-jk_0r_0}-1)-\frac{1}{jk_0}r_0e^{-jk_0r_0}], \qquad (9)$$

where $r_0=\sqrt[3]{\frac{3\Delta V}{4\pi}}$ is the radius of the sphere whose volume is equal to the ΔV of the cube volume.

Along with the development of computer technology, as for the solving of matrix equation (8), there have been brought forward numerous fast algorithms towards the matrix equation solving. Fast algorithms which are frequently used, includes Fast Multipole Method (FMM) [14] and its extension, the Multilevel Fast Multipole Algorithm (MLFMA) [15], Conjugate Gradient Gast Fourier Transform method (CG-FFT) [16], the Adaptive Integral Method (AIM) [17], etc.; which are all being obtained with widely application. This paper adopts stable BCG-FFT method [18], which provides the solving of the aspects of electromagnetic inverse scattering with high-performance unitary algorithm, along with the effective reduction of memory requirements and computation time of computer.

III. SVM-BASED INVERSE SCATTERING PROCEDURE

Generally speaking, a regression problem is the process through when an unknown function f is approximated by means of a function $\overline{f}$ on the basis of some sample $\left\{(\underline{v}_n,e_n)\right\}_{n=1,\dots,N}$, being $\underline{v}_n$ an input pattern and e_n the corresponding target $(e_n=f\left\{\underline{v}_n\right\})$. As far as parameters reconstruction of composite conducting-dielectric object are concerned, the dimension (r) and the complex permittivity (ε_r,σ) of the scatter must be retrieved and each unknown parameters is dealt with separately. Consequently, $\underline{v}_n=(\underline{E}^s)_n$ and $e_n=(\chi_i)_n$.

SVM is a new paradigm that have been recently proposed for the solution of pattern recognition and function approximation tasks. Briefly (the reader can refer to [19] for more details), the SVM-based procedure aim at finding a smooth function $\overline{f}$ that approximates f while keeping at most, a deviation ε from the targets e_n for all samples. Thus, f is approximated in a linear way:

$$\overline{f}(\underline{v}) = w \cdot \Phi(\underline{v_n}) + c\,, \tag{10}$$

where w represents the vector of weights of the linear function, $\Phi(\cdot)$ is the mapping that projects the samples from the original into the higher dimensional feature space and c is the bias.

The optimal linear function in the transformed space is selected by minimizing the structural risk, which is the combination of the training error (empirical risk) and the model complexity (confidence term). The first term is calculated according to a $\varepsilon-$ insensitive loss function and can be expressed by means of nonnegative slack variables ξ and ξ^*, which measure the distance (in the target space) of the training samples lying outside the $\varepsilon-$ insensitive tube from the tube itself. The second term of the cost function is expressed through the Euclidean norm of the weight vector w, which can be inversely related to the geometrical margin of the corresponding solution and thus, to the complexity of the model. The cost function to minimize becomes:

$$\Psi(w,\xi) = C\sum_{n=1}^{N}(\xi+\xi^*) + \frac{1}{2}\|w\|^2\,, \tag{11}$$

subjected to the following constraints:

$$\begin{cases} e_n - [w\cdot\Phi(\underline{v_n}) + c] \le \varepsilon + \xi_n, \\ [w\cdot\Phi(\underline{v_n}) + c] - e_n \le \varepsilon + \xi_n^*, \quad n = 1,2,\ldots,N, \\ \xi_n, \xi_n^* \ge 0, \end{cases} \tag{12}$$

C is a regularization parameter that allows one to tune the tradeoff between the complexity (or flatness) of the function $\overline{f}$ and the tolerance to empirical errors.

The constrained optimization problem in (11) can be reformulated through a Lagrange function, which leads in the dual formulation to a Convex Quadratic Problem (CQP) and thus, to a unique solution (the global minimum of the cost function). The final prediction function in terms of the samples in the original input domain, becomes:

$$\overline{f}(\underline{v}) = \sum_{n\in N}(\alpha_n - \alpha_n^*)k(\underline{v_n},\underline{v}) + c\,, \tag{13}$$

where α_n and α_n^* represent the Lagrange multipliers of the CQP and $k(.,.)$ is a kernel function, which allows one to evaluate the similarity between a pair of sample in the transformed feature space as a function of the samples in the input space. The commonly adopted kernels are polynomial and Gaussian Radial Basis Function (RBF) kernels. In SVM, the samples associated with a nonzero Lagrange multiplier are called support vectors, the other samples have no weight in the definition of the result since they fall within the $\varepsilon-$ tube. The CQP problem can be solved using standard optimization techniques. In this work, a very effective procedure, Sequential Minimal Optimization (SMO) [20] is adopted. The parameter c can be computed by means of the Karush-Kuhn-Tucker conditions of the CQP at optimality [19].

Some attractive features of the SVM result from the analytical formulation presented earlier and are as follows [21]:

1) Good intrinsic generalization ability, owing to the use of the $\varepsilon-$ insensitive cost function and the optimization of both empirical error and model complexity to drive learning process;
2) Limited complexity and high stability of the learning process, due to the convexity of the optimization problem and the use of the kernel trick;
3) Ease of use, since relativity few free parameters (or hyperparameters; i.e., the regularization coefficient C, the width of the insensitive tube ε and the kernel types and parameters) have to be tuned.

IV. NUMERICAL RESULTS

A. The electromagnetic scattering of composite conducting-dielectric objects

In order to prove the correctness, two valuable objects of two-dimension metal/dielectric composite structure are considered by BCG-FFT method and making comparison with the FDTD method.

1) Inhomogeneous medium covering conducting cylinder.

A unit TM plane wave reflects upon the indefinite medium covering conductor cylinder along X-axis (suppose the cylinder axis is Z-axis), the radius of conductor is 0.2λ and the thickness of medium is 0.1λ ; two kinds constitute the medium and the relative dielectric constants are $\varepsilon_{r1} = 4.0$, $\varepsilon_{r2} = 20.0$, respectively. Medium 1 locates under X-axis, which medium 2 is above X-axis. Figure 1 provides with the bistatic Radar Cross Section (RCS) σ of the object (using normalization of wavelength). The result obtained by FDTD also shown in the figure, which indicates good correspondence with the result of the approach above. It is worth noting that some deviation are shown in the range of $200^0 - 300^0$. This can be explained in the following two aspects: first, the relative simple substitute of rectangle to cube, which may cause deviation and the another may result from the process of central point matching.

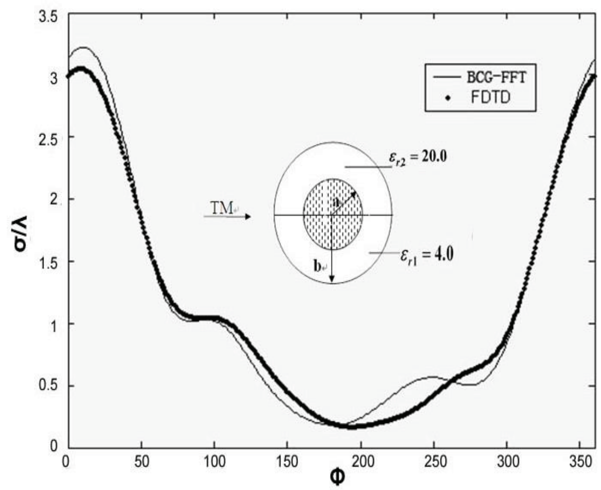

Fig. 1. Bistatic RCS of a conducting cylinder ($ka = 1.256$) with a inhomogeneous coating ($kb = 1.884$, $\varepsilon_r = 4.0$ and 20.0).

2) Metal-medium constituting the compound square column.

A unit TM plane wave reflects into the object of metal/medium composite square column, the angle of arrival is $\varphi = 270^0$, half the object is a conductor (left), while half the object is a medium (right); both of the cross sections of the metal and the medium are squares with the length of a side 0.2λ and the relative permittivity is 4.0. Figure 2 puts up the σ of the object. It's obtained result matches with the result of the document [22] and Fig. 2 also provides with the computing result of FDTD.

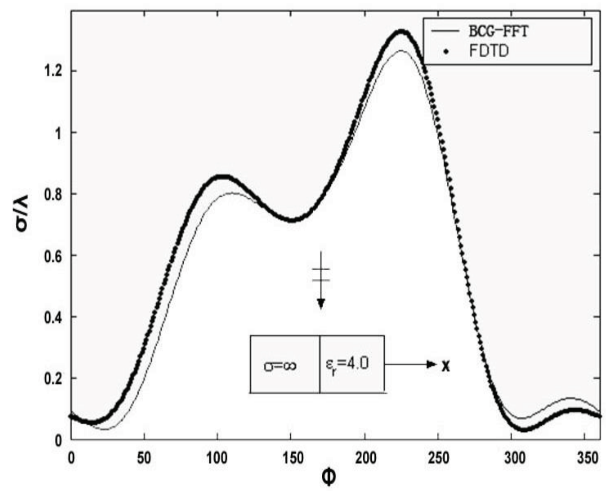

Fig. 2. Bistatic RCS of a composite conducting dielectric square column with the length of side 0.2λ and relative permittivity 4.0.

B. The reconstruction of composite conducting-dielectric cylinder

1) The reconstitution of the relative permittivity ε_r and the medium covering thickness b.

A unit TM plane wave ($f = 1GHz$) vertically reflects into the lossless medium covering conductor cylinder (Fig. 3) with its inside radius and outer radius are a and b, respectively; $a = \lambda/6$, suppose the values range of b is at [7, 23] cm, while the values range of ε_r is at [1.5, 5.0]. In the "learning phase", a data set of 135 examples: $\varepsilon_r = 1.5 + 0.25n,\ n = 0,1,...,14,\quad b = 7.0 + 2n(cm),$ $n = 0,1,...,8$, is considered and defined a suitable set to train SVM for the reconstruction problems. Because SVM has been developed to solve one-output learning problems [19], two different SVMs, one for the reconstitution of the relative permittivity ε_r and the other for the reconstitution of the medium covering thickness b are trained by using the SMO algorithm. Gaussian RBF kernel (with kernel width γ^2) are considered as kernel functions, due to their capability to work as universal approximator [11]. In order to obtain the scattering electric field of objective truly and perfectly, we place 12 observation points of scattered filed, which evenly distribute at the distance from the circular arc with the center radius of λ and the length of $3\pi\lambda/2$, just as Fig. 3 shows. The sample information are all the amplitude of scattered field of observation point, which can directly get by the analytic method. After proper trained, the values of the hyperparameters of the SVM are given in Table 1.

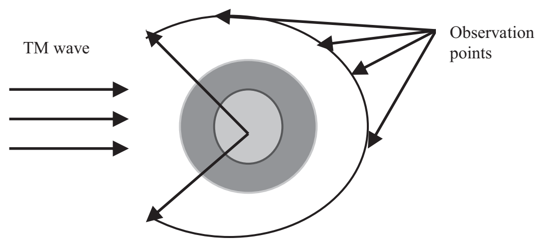

Fig. 3. Conductor cylinder coated with dielectric material illuminated by a plane wave.

Table 1: The values of the SVM hyperparameters

	ε	C	γ^2
ε_r	0.001	999.8545	0.2460
b	0.001	1004.6867	0.2441

In order to compare SVM and NN performances under the same "conditions", the same training set has been considered during the NN training phase. In this studies, the network structure having 12 input ports, 12 nodes in the hidden layer and 2 output ports (means 12-12-2 network) is considered. In training phase, a Backpropagation algorithm is used to train the NN (BPNN) in this work.

The performances of the BPNN and SVM-based procedure are illustrated and compared by considering a test set made up of 96 examples ($\varepsilon_r = 1.55, 1.80, 2.05, 2.30, 2.55, 2.76, 3.05, 3.30, 3.80,$ $4.50, 4.55, 4.90$; $b = 8.0 + 2n(cm)$, $n = 0,1,...,7$). The relative permittivity ε_r and radius b are different from those of the training set. Figures 4 and 5 show the estimated versus the actual scatterer properties when the SVM-based and BPNN-based approaches are taken into account, respectively.

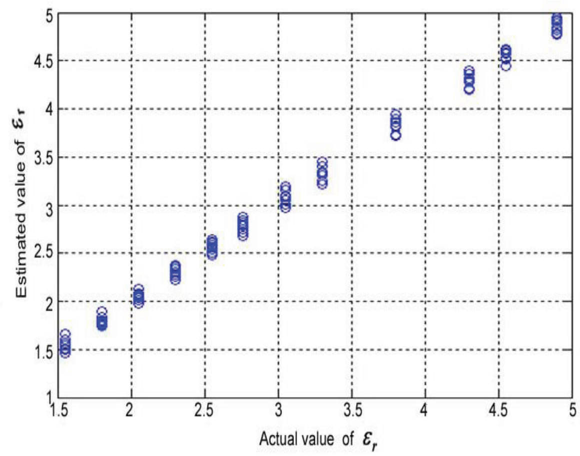

(a)

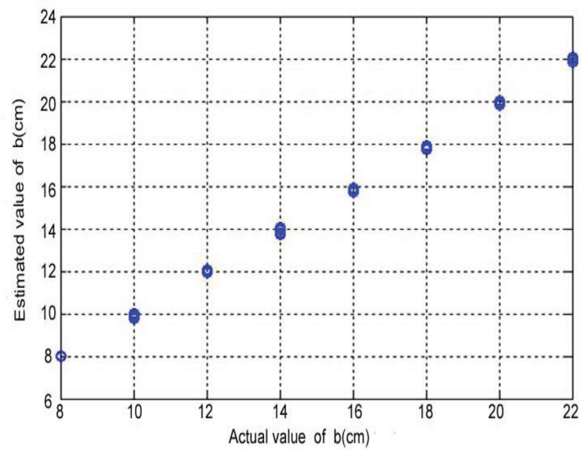

(b)

Fig. 4. SVM-based approach. Estimated versus real scatterer properties: (a) ε_r and (b) b.

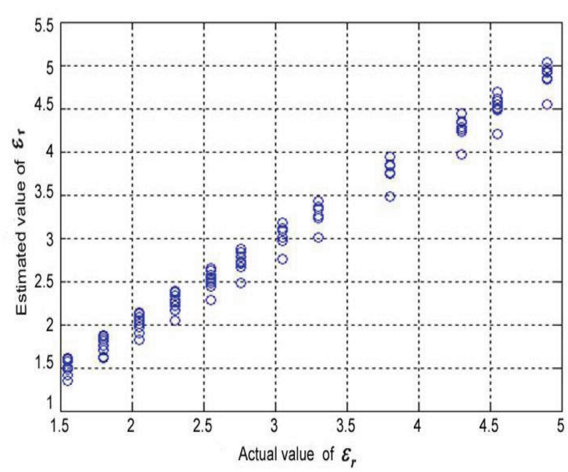

(a)

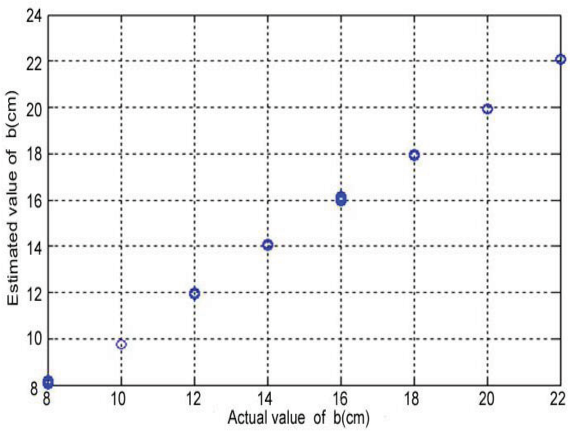

(b)

Fig. 5. BPNN-based approach (12-12-2). Estimated versus real scatterer properties: (a) ε_r and (b) b.

Results of the reconstruction errors are summarized in Table 2, where the Maximum Absolute Error (MAE), Average Absolute Error (AAE), Maximum Relative Error (MRE) and Average Relative Error (ARE) achieved in the reconstruction are listed. As can be seen, reconstruction results are very good, since both the relative permittivity and the medium covering thickness are reconstructed with an average relative error less than 2%. Comparison of the performance of the 12-12-2 network is carried out by examining the results summarized in Table 3. As expected, SVM enhances the performances achieved with the BPNN approach, due to the solution of the CQP problems.

Table 2: Errors in the reconstruction of ε_r and b achieved by using the SVM

	MAE	AAE	MRE	ARE
ε_r	0.1518	0.0532	7.20%	1.88%
b	0.2992	0.0835	2.31%	0.57%

Table 3: Errors in the reconstruction of ε_r and b achieved by using the BPNN (12-12-2)

	MAE	AAE	MRE	ARE
ε_r	0.3494	0.0900	12.87%	3.27%
b	0.2601	0.0972	2.74%	0.83%

2) The reconstitution of the relative permittivity ε_r, the medium covering thickness b and the conductivity σ.

In this example, the installation of incident wave, objects and observation points shares the same as the last example. The total number of training samples is 800 and the training set's variation rules are: $\varepsilon_r = 1.5 + 0.4n, n = 0,1,...,9$, $b = 8.0 + 2.0n\,(cm)$, $n = 0,1,...,7$ and $\sigma = 10^{-3+0.1n}\,(S/m), n = 0,1,...,9$, respectively. After training phase, the values of the hyperparameters are given in Table 4.

Table 4: The values of the SVM hyperparameters

	ε	C	γ^2
ε_r	0.001	1001.8193	0.1665
b	0.01	1000.1480	0.1667
σ	0.00001	10000	0.2512

Results refer to the processing of a test set made up of 216 examples that do not belong to the training set: $b = 9.0 + 2n\,(cm), n = 0,1,...,5$; $\varepsilon_r = 1.65, 2.05, 2.5, 3.3, 4.0, 4.9$; $\sigma = 10^{-t}\,(S/m)$, $t = 2.95, 2.81, 2.75, 2.55, 2.35, 2.15$. The sample information is the amplitude of scattering field of observation points, we can get it with BCG-FFT method. Figure 6 shows the estimated versus the actual scatterer properties. Table 5 shows the results of the reconstruction errors. Under the same conditions, similar results have been obtained also when the BPNN (12-12-3) approach is adopted for reconstruction problems and are given in Table 6.

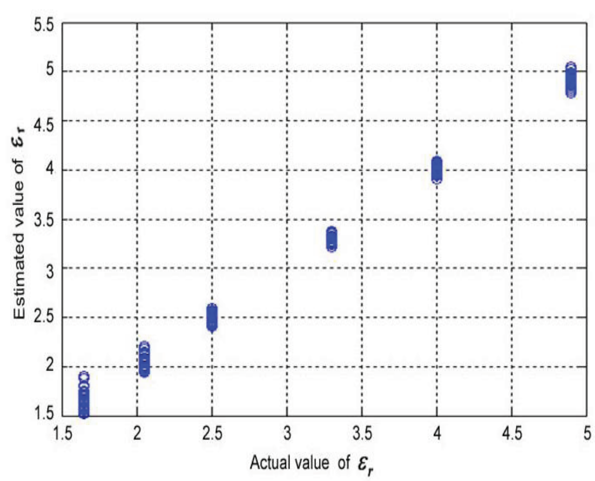

(a)

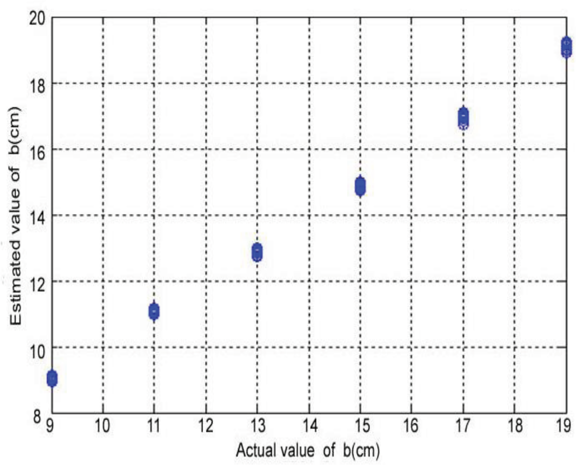

(b)

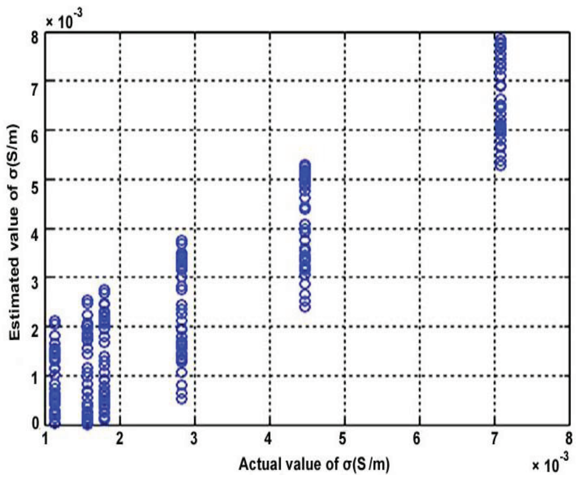

(c)

Fig. 6. SVM-based approach. Estimated versus real scatterer properties: (a) ε_r, (b) b and (c) σ.

Table 5: Errors in the reconstruction of ε_r 、 b and σ achieved by using the SVM

	MAE	AAE	MRE	ARE
ε_r	0.2032	0.0533	12.32%	1.92%
b	0.2004	0.0727	1.82%	0.56%
σ	0.0020	5.3987e-4	181.48%	25.81%

Table 6: Errors in the reconstruction of ε_r 、 b and σ achieved by using the BPNN (12-12-3)

	MAE	AAE	MRE	ARE
ε_r	0.2550	0.0531	15.45%	2.15%
b	0.2900	0.1001	2.23%	0.74%
σ	0.0023	7.8362e-4	99.61%	34.46%

Figure 6 shows the estimated versus the actual scatterer properties when the SVM-based approach is taken into account. As for the reconstruction of relative permittivity ε_r and the medium covering thickness b, from Tables 5 and 6, both of those two methods result sound; what's more, SVM method has an advantage over BPNN method. However, both of those methods also result in big relative errors during the reconstruction of the conductivity σ. It is possible that the big error just corresponds to the small actual value according to theoretical analysis.

V. CONCLUSION

In this letter, an innovative inverse scattering methodology, based on the implementation of a support vector machine has been presented and applied to the reconstruction of composite conducting-dielectric objects. The samples data fed to the SVM are the amplitude of scattered fields from composite conducting-dielectric objects collected at some receiving points and obtained by using the BCG-FFT method. The training of SVM requires the solution of a constrained quadratic optimization problem. This is a key point of the proposed approach, which can overcome the typical drawbacks as over-fitting or local minima occurrence (with respect to NN). The efficiency of the proposed technique was illustrated in the case of the reconstruction of geometric and dielectric properties of composite conducting-dielectric objects. Some numerical results validate the accuracy and efficiency of the method by comparing with the BPNN method.

ACKNOWLEDGMENT

This work was supported by the National Natural Science Foundation of China (No. 61179025) and the Natural Science Foundation of Hubei Provincial Department of Education (No. D20111201).

REFERENCES

[1] S. M. Rao, C. C. Cha, R. L. Cravey, and D. L. Wilkes, "Electromagnetic scattering from arbitrary shaped conducting bodies coated with lossy materials of arbitrary thickness," *IEEE Trans. Antennas Propag.*, vol. 39, no. 5, pp. 627-631, 1991.

[2] T. K. Sarkar and E. Arvas, "An integral equation approach to the analysis of finite microstrip

antennas: volume/surface formulation," *IEEE Trans. Antennas Propag.*, vol. 38, no. 3, pp. 305-313, 1990.

[3] C. C. Lu and W. C. Chew, "A coupled surface-volume integral equation approach for the calculation of electromagnetic scattering from composite metallic and material targets," *IEEE Trans. Antennas Propag.*, vol. 48, no. 12, pp. 1866-1868, 2000.

[4] X. C. Nie, N. Yuan, L. W. Li, Y. B. Gan, and T. S. Yeo, "A fast volume-surface integral equation solver for scattering from composite conducting-dielectric objects," *IEEE Trans. Antennas Propag.*, vol. 53, no. 2, pp. 818-823, 2005.

[5] M. A. Carr, E. Topsakal, J. L. Volakis, and D. C. Ross, "Adaptive integral method applied to multilayer penetrable scatterers with junctions," *In IEEE Antennas Propag. Soc. Int. Sypm.*, pp. 856-861, 2001

[6] R. Mydur and K. A. Michalski, "A neural network approach to the electromagnetic imaging of elliptic conducting cylinders," *Microwave Opt. Technol. Lett.*, vol. 28, no. 5, pp. 303-306, 2001.

[7] I. T. Rekanos, "On-line inverse scattering of conducting cylinders using radial basis-function neural networks," *Microwave Opt. Technol. Lett.*, vol. 28, no. 6, pp. 378-380, 2001.

[8] E. Bermani, S. Caorsi, and M. Raffetto, "An inverse scattering approach based on a neural network technique for the detection of dielectric cylinders buried in a lossy half-space," *PIER*, vol. 26, pp. 67-87, 2000.

[9] E. Bermani, S. Caorsi, and M. Raffetto, "Microwave detection and dielectric characterization of cylindrical objects from amplitude-only data by means of neural networks," *IEEE Trans. Antennas Propag.*, vol. 50, no. 9, pp. 1309-1314, 2002.

[10] E. Bermani, S. Caorsi, and M. Raffetto, "Geometric and dielectric characterization of buried cylinders by using simple time-domain electromagnetic data and neural networks," *Microwave Opt. Technol. Lett.*, vol. 24, no. 1, pp. 24-31, 2000.

[11] E. Bermani, A. Boni, S. Caorsi, and A. Massa, "An innovation real-time technique for buried object detection," *IEEE Trans. Geosci. Remote Sens.*, vol. 41, no. 4, pp. 927-931, 2003.

[12] Q. H. Zhang, B. X. Xiao, and G. Q. Zhu, "Inverse scattering by dielectric cylinder using support vector machine approach," *Microwave Opt. Technol. Lett.*, vol. 49, no. 2, pp. 372-375, 2007.

[13] V. Vapnik, "Statistical learning theory," *New York: Wiley*, 1998.

[14] R. Coifman, V. Rokhlin, and S. Wandzura, "The fast multipole method for the wave equation: a pedestrian prescription," *IEEE Antennas Propag.*, vol. 35, pp. 7-12, 1993.

[15] J. M. Song, C. C. Lu, and W. C. Chew, "Multilevel fast-multipole algorithm for electromagnetic scattering by large complex objects," *IEEE Trans. Antennas Propag.*, vol. 45, no. 10, pp. 1488-1493, 1997.

[16] T. K. Sarkar, E. Arvas, and S. M. Rao, "Application of FFT and conjugate gradient method for the solution of electromagnetic radiation from electrically large and small conducting bodies," *IEEE Trans. Antennas and Propagate.*, vol. 34, no. 5, pp. 635-640, 1986.

[17] E. Bleszynski, M. Bleszynski, and T. Jaroszewicz, "AIM: adaptive integral method for solving large scale electromagnetic scattering and radiate on problems," *Radio Sci.*, vol. 31, pp. 1225-1251, 1996.

[18] X. M. Xu, Q. H. Liu, and Z. Q. Zhang, "The stabilized biconjugate fradient fast fourier transform method for electromagnetic scattering," *J. Appl. Computat. Electromagn.*, vol. 17, no. 1, pp. 97-103, 2002.

[19] N. Cristianini and J. S. Taylor, "An introduction to support vector machine," *Cambridge Univ. Press*, Cambridge, U.K., 2000.

[20] J. Platt, "Fast training of support vector machine using sequential minimal optimization," *In: B. Scolkopf, C. Burges, and A. Smola (Eds.)*, "Advances in kernel methods-support vector learning," *MIT Press*, Cambridge, MA, 1999.

[21] L. Pasolli, C. Notarnicola, and L. Bruzzone, "Estimating soil moisture with the support vector regression technique," *IEEE Geoscience and Remote Sensing Letters*, vol. 8, no. 6, pp. 1080-1084, 2011.

[22] A. Z. Elsherbeni and A. A. Kishk, "Modeling of cylindrical objects by circular dielectric and conducting cylinders," *IEEE Trans. Antennas and Propag.*, vol. 40, no. 1, pp. 96-99, 1992.

Zhang Qing-he (S ' 92-M ' 07) received his B.S. degree from the Central China Normal University, Wuhan, China, and his Ph.D. degrees from the Wuhan University, Wuhan, China, in 1992 and 2007, respectively; both in Radio Physics. Since 2007 he has been with the School of Science of the China Three Gorges University as an Associate Professor. His research interests include microwave remote sensing of the sea and land surface, computational electromagnetics and application of neural networks and fuzzy systems in inversion problems.